

Refining Latent Homophilic Structures over Heterophilic Graphs for Robust Graph Convolution Networks

Chenyang Qiu¹, Guoshun Nan^{1*}, Tianyu Xiong¹, Wendi Deng¹, Di Wang¹, Zhiyang Teng², Lijuan Sun¹, Qimei Cui¹, Xiaofeng Tao¹

¹Beijing University of Posts and Telecommunications, China

²Nanyang Technological University, Singapore

{cyqiu, nanguo2021, tyxiong, dengwendi, wdwdwd, sunlijuan, cuiqimei, taoxf}@bupt.edu.cn, chihyangteng@gmail.com

Abstract

Graph convolution networks (GCNs) are extensively utilized in various graph tasks to mine knowledge from spatial data. Our study marks the pioneering attempt to quantitatively investigate the GCN robustness over omnipresent heterophilic graphs for node classification. We uncover that the predominant vulnerability is caused by the structural out-of-distribution (OOD) issue. This finding motivates us to present a novel method that aims to harden GCNs by automatically learning Latent Homophilic Structures over heterophilic graphs. We term such a methodology as **LHS**. To elaborate, our initial step involves learning a latent structure by employing a novel self-expressive technique based on multi-node interactions. Subsequently, the structure is refined using a pairwise constrained dual-view contrastive learning approach. We iteratively perform the above procedure, enabling a GCN model to aggregate information in a homophilic way on heterophilic graphs. Armed with such an adaptable structure, we can properly mitigate the structural OOD threats over heterophilic graphs. Experiments on various benchmarks show the effectiveness of the proposed LHS approach for robust GCNs.

Introduction

Graph-structured spatial data, such as social networks (Qiu et al. 2022b) and molecular graphs, is ubiquitous in numerous real-world applications (Li et al. 2022). Graph convolution networks (GCNs) (Kipf and Welling 2017), following a neighborhood aggregation scheme, are well-suited to handle these relational and non-Euclidean graph structures, and have been widely applied in various graph tasks, including node classification and recommender systems. Recently, there has been a surge in GCN approaches for challenging heterophilic graphs (Zhu et al. 2020a), where most neighboring nodes have different labels or features. These methods can be divided into two categories: 1) Multi-hop-based approaches (Abu-El-Haija et al. 2019; Jin et al. 2021a; Wang and Derr 2021); 2) Ranking-based approaches (Liu, Wang, and Ji 2021; Yuan and Ji 2021; Yang et al. 2022). The former group learns node representations based on multi-hop aggregations, while the latter performs selective node aggregations by a sorting mechanism. These GCN methods continue to advance the state-of-the-art performance for node classification and have enabled various downstream applications (Lin, Lan, and Li 2021; Qiu et al. 2023).

*Guoshun Nan is the corresponding author.
Copyright © 2024, Association for the Advancement of Artificial Intelligence (www.aaai.org). All rights reserved.

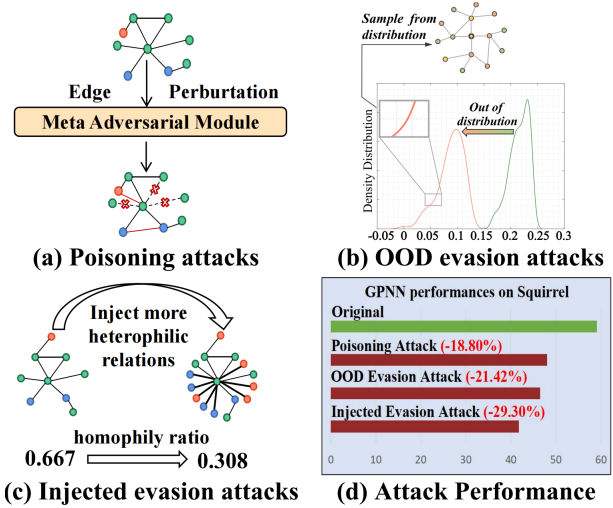


Figure 1: Illustration for the vulnerability of existing GPNN under various threats on Squirrel, including a poisoning attack, and another two adapted from evasion attacks. The sub-figures (a), (b), and (c) depict how we generate the above three attacks, and (d) reports the significant performance degradation under each attack.

gations by a sorting mechanism. These GCN methods continue to advance the state-of-the-art performance for node classification and have enabled various downstream applications (Lin, Lan, and Li 2021; Qiu et al. 2023).

Despite the significant success of the current GCN methods on heterophilic graphs, these approaches are **extremely vulnerable to malicious threats** that aim to distort the structure of the target graph during testing. We conduct experiments to attack the state-of-the-art GPNN (Yang et al. 2022) method, which was trained on the popular Squirrel (Pei et al. 2020) benchmark for heterophilic graphs, using samples created by various attacks. Fig.1 demonstrates that the accuracy of node classification can be greatly reduced under three different types of destructive attacks, including a well-known poisoning attack (Jin et al. 2020), and two attacks adapted from evasion attacks (Biggio et al. 2013; Zhang et al. 2016). Specifically, as shown in Fig.1 (a), the poisoning attack produces adversarial structural perturbations to the edges of the graph, fooling GPNN to make incor-

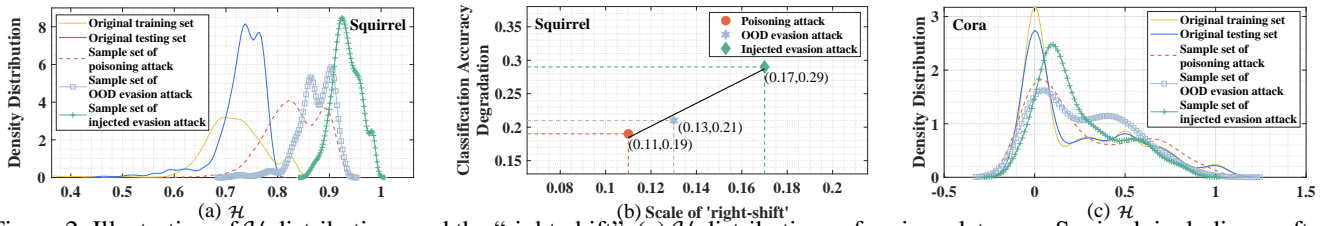


Figure 2: Illustration of \mathcal{H} distributions and the “right-shift”. (a) \mathcal{H} distributions of various data over Squirrel, including crafted sample sets of three attacks. (b) correlation between the “right-shift” of \mathcal{H} distributions and node classification degradation. (c) \mathcal{H} distributions of various data, including the original train and test set of a homophilic dataset Cora, and crafted sample sets of three attacks.

rect predictions. The proposed two evasion-based attacks are referred to as “OOD evasion attacks” and “injected evasion attacks”, respectively. Fig.1 (b) and Fig.1 (c) demonstrate how the sample sets for these two attacks are created. The first generates a graph with a node distribution that is vastly different from that of the target testing set, while the second manipulates the target graph by injecting more heterophilic edges. Under these three attacks, Fig.1 (d) shows that classification accuracy of GPNN is sharply decreased by 18.90%, 21.42%, and 29.30%, respectively.

To analyze the reasons why GCN methods are fragile on heterophilic graphs, we further depict the \mathcal{H} distributions (Zheng et al. 2022) of the crafted data from the aforementioned three attacks, as well as the distributions of the original train and test sets of Squirrel in Fig.2 (a). Here \mathcal{H} represents the node-level heterophily, which is the proportion of a node’s neighbors that have a different class¹. Fig.2 (a) demonstrates that the distributions of three attack samples are all located to the right of the training set, with the most destructive sample for the GPNN method being the furthest to the right. This observation led us to investigate the correlation between the “right-shift” of the \mathcal{H} distribution relative to the train set and the vulnerability of GCN approaches. This correlation is visualized in Fig.2 (b) and it is shown that the scale of “right-shift” is strongly proportional to the degradation of node classification performance. We refer to this phenomenon as “**structural out-of-distribution (OOD)**” in GCN methods for graphs of spatial data.

To investigate the underlying cause of the aforementioned structural OOD, we attacked another GPNN model that was trained on the homophilic graph Cora (Yang, Cohen, and Salakhudinov 2016) and depicted the resulting \mathcal{H} distributions in Fig.2 (c). Interestingly, the shifts of the three attacks relative to the training set of Cora are very small. This minor “right-shift” enables the GPNN model trained on Cora to be more robust. We attribute this to the strong homophily present in the Cora dataset and believe that more homophily will result in less “right-shift” under attacks, even for heterophilic graphs, and hence alleviate the structural OOD.

In light of the above discussion, a critical question arises: “How can a GCN model automatically learn an appropriate **homophilic structure over heterophilic graphs** to reduce the scale of “right-shift” in \mathcal{H} distributions?” This could help to make the model more resistant to malicious attacks

¹A more formal definition is given in Preliminaries Section, and higher \mathcal{H} values indicate a node with strong heterophily.

on heterophilic graphs. Achieving this goal is challenging. Despite the success of many structure learning-related methods (Jin et al. 2021b,a; He et al. 2022), they also tend to strengthen the heterophily or only focus on the *local* relations between two nodes rather than considering the *global* connections. These methods still suffer from vulnerability issues under attacks (as seen in Figure 4 and Table 1), and they are hardly able to address the challenge.

We address the above challenging question with a novel method called LHS. The key components of the proposed LHS are: 1) a self-expressive generator that automatically induces a latent homophilic structure over heterophilic graphs via multi-node interactions, and 2) a dual-view contrastive learner that refines the latent structure in a self-supervised manner. LHS iteratively refines this latent structure during the learning process, enabling the model to aggregate information in a homophilic way on heterophilic graphs, thereby reducing the “right-shift” and increasing robustness. It should be noted that the original graph Experiments on five benchmarks of heterophilic graphs show the superiority of our method. We also verify the effectiveness of our LHS on three public homophilic graphs. Additionally, the induced structure can also be applied to other graph tasks such as clustering. Our contributions are as follows:

- We quantitatively analyze the robustness of GCN methods over omnipresent heterophilic graphs for node classification, and reveal that the “right-shift” of \mathcal{H}_{node} distributions is highly proportional to the model’s vulnerability, i.e., the structural OOD. To the best of our knowledge, this is the first study in this field.
- We present LHS, a novel method that strengthens GCN against various attacks by learning latent homophilic structures on heterophilic graphs.
- We conduct extensive experiments on various spatial datasets to show the effectiveness of the proposed LHS in mitigating the structural OOD issue.

Related Work

Graph Convolution Networks

There is a line of early studies in graph convolution networks (GCNs) (Kipf and Welling 2016, 2017; Hamilton, Ying, and Leskovec 2017; Veličković et al. 2018). Recent GCN approaches over heterophilic graphs can be grouped into multi-hop-based ones (Abu-El-Haija et al. 2019; Zhu et al. 2020a; Jin et al. 2021b; Wang and Derr 2021; Wang et al. 2022b), ranking-based ones (Liu, Wang, and Ji 2021; Wang et al.

2022a; Yang et al. 2022), and the ones using GCN architecture refinement (Bo et al. 2021; Yang et al. 2021; Suresh et al. 2021a; Yan et al. 2021; Luan et al. 2022; Xu et al. 2023; Li, Kim, and Wang 2023; Zheng et al. 2023). These methods have achieved remarkable success in graph node classification. However, robustness is yet to be explicitly considered on challenging heterophilic graphs.

Robust Graph Convolution Networks

Recently we have witnessed a surge in the robustness of GCN on heterophilic graphs. These methods can be categorized into the structure learning-based ones (Jin et al. 2020, 2021a; He et al. 2022; Zhu et al. 2022; Liu et al. 2023), and the ones based on adversarial training (Dai et al. 2018; Zhu et al. 2019; Zhang, Zhang, and Cheng 2020; Zhang and Zitnik 2020; Suresh et al. 2021b). The most related to our work is ProGNN (Jin et al. 2020) which explores the low-rank and sparsity of the graph structure, and SimP-GCN (Jin et al. 2021b) which relies on a similarity preservation scheme for structure learning. Our work differs from the above methods in two aspects: 1) We focus on the structural OOD issue of GCN approaches over heterophilic graphs. To the best of our knowledge, this problem is largely ignored in previous works. 2) We iteratively refine the latent structure of heterophilic graphs by a novel self-expressive method and a dual-view contrastive learning scheme, enabling a GCN model to effectively aggregate information in a homophilic way on heterophilic graphs.

Preliminaries

We denote the graph as $G = (V, E, \mathbf{X})$, where $V \in \mathbb{R}^{N \times N}$ is the set of nodes, E is the set of edges between nodes, \mathbf{X} is the node features and (V, E) can form the original network structure \mathbf{A} . We aim to generate a latent homophilic structure for robust GCN in node classification. For convenience, we give the following edge definition:

Definition 1. (Positive/Negative Edge) A **positive** edge indicates that the two nodes in the link have the same type, while **negative** one refers to a link that connects two nodes with different types.

Node-level Heterophily: We use \mathcal{H} to represent the node-level heterophily, which is the proportion of a node’s neighbors that have a different class. We refer to (Zheng et al. 2022) to give a formal definition, and it is a fine-grained metric to measure the edge heterophily in a graph.

Definition 2. Node-level Heterophily (\mathcal{H}):

$$\mathcal{H}(v_i) = \frac{|(v_i, v_j) \mid y(v_i) \neq y(v_j)|}{|\mathcal{E}(v_i)|}, \forall v_i, v_j \in V, \quad (1)$$

where $(v_i, v_j) \in \mathcal{E}(v_i)$, $\mathcal{E}(v_i)$ is the edge set of v_i , $y(v_i)$ is the node class of v_i , and $|\cdot|$ represents the number of edges. The nodes with strong heterophily have higher \mathcal{H} (closer to 1), whereas nodes with strong homophily have smaller \mathcal{H} (closer to 0). It also provides an edge distribution sampling set for quantitative analysis over heterophilic graphs.

OOD Formulation: We rigorously formulate the ego-graph edge distribution by utilizing the proposed node-level heterophily, and the formulation further enables the multi-layer

edge distribution analyses. The ‘right-shift’ phenomenon found in the heterophilic graphs also motivates us to propose latent homophilic structure refinement. Theoretical analysis from a spectral-domain view is given in Appendix 1² to further elaborate the rationale of the proposed LHS.

Edge Distribution Formulation: Given a random node $v_i \in V$, we define v_i ’s k -hop neighbors as $N_{v_i}(k)$ (where k is an arbitrary positive integer) and the nodes in $N_{v_i}(k)$ form an ego-graph substructure called $A_{v_i}(k)$, which consists of a local adjacency matrix represented as $A_{v_i}(k) = \{a_{v_i u} \mid u \in N_{v_i}(k)\}$. In this way, we can study the distribution of the k -hop substructure A_v via $p(\mathcal{H} \mid A_{v_i}(k)) = p(\mathcal{H} \mid A_{v_i}(1)A_{v_i}(2)\dots A_{v_i}(k))$. It’s worth noting that the ego-graph can be seen as a Markov blanket for the centered node v_i , meaning that the conditional distribution $p(\mathcal{H} \mid A_{v_i}(k))$ can be decomposed as a product of independent and identical marginal distributions $p(\mathcal{H} \mid A_{v_i}(i), i \in k)$ for each of the $A_{v_i}(j), j \leq k$. We also provide more empirical observations about the ‘‘right-shift’’ phenomenons on heterophilic graphs, which are available in Appendix 3.

Methodology

Overview

In this section, we present the proposed LHS. Our goal is to learn an appropriate latent homophilic structure from heterophilic graphs, so as to reduce the scale of ‘‘right-shift’’ in \mathcal{H} distributions. Inspired by the analysis in the Introduction Section that more homophily of a graph can reduce the ‘‘right-shift’’, our latent structure tends to encourage positive edge connections by increasing the edge weights for pairs of nodes with the same type, and suppresses negative edge connections by reducing the edge weight for nodes with different types. Fig. 3 shows the architecture of LHS.

Structure Inducer

The proposed structure inducer involves a self-expressive generator and a dual-view contrastive learner.

Self-Expressive Generator. Our proposed self-expressive generator produces a latent homophilic structure over heterophilic graphs in three steps:

Step 1: Capturing multi-node information. Given the node features \mathbf{X} , we aim to capture the multi-node feature information by expressing one node feature via a linear or affine combination of other node features. Differently from the existing structure learning method with pair-wise similarity matrix (Jin et al. 2021a), our inducer can generate fine-grained latent structure $S^* \in \mathbb{R}^{N \times N}$ by discovering the global information in low-dimension subspace. Specifically, for $\forall v_i \in V$, we express it by a linear sum of multi-node features $\mathbf{x}_j, v_j \neq v_i$, which can be expressed as $\mathbf{x}_i = \sum_{v_j \in V} q_{ij} \mathbf{x}_j$, where q_{ij} is the (i, j) th element of a coefficient matrix Q .

Step 2: Optimizing the generator loss. We use the coefficient matrix Q to generate latent structure. The optimization problem to solve Q can be formulated as follows:

$$\min_Q \|Q\|_F \quad s.t. \quad \mathbf{X} = Q\mathbf{X}; \text{diag}(Q) = 0 \quad (2)$$

²Appendices are available in the preprint version.

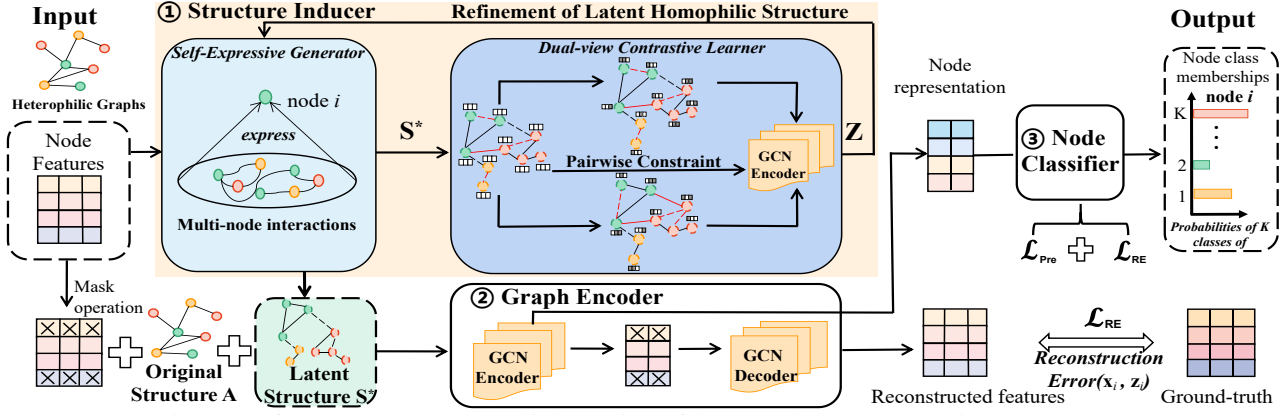


Figure 3: The architecture of the proposed LHS, which consists of three modules: structure inducer, graph encoder, and node classifier. The key ingredient structure inducer involves two components, i.e., the self-expressive generator and dual-view contrastive. The former learns a latent homophilic structure by multi-node interactions and then the latter refines the structure. We iteratively perform such a procedure to learn a better homophilic structure on heterophilic graphs. The refined structure will be fed to the graph encoder for representation aggregation, and finally, the classifier for node classification.

where $\|Q\|_F$ is the Frobenius matrix norm (Böttcher and Wenzel 2008) of Q and $\text{diag}(Q)$ denotes the diagonal entries of Q . Eq. 2 optimizes a block-diagonal matrix Q to generate the latent structure S^* . Each block of Q contains the nodes which belong to the same class, thus mitigating the “right-shift” phenomenon. We relax the hard constraint $\mathbf{X} = Q\mathbf{X}$ with a soft constraint $(\mathbf{X} - Q\mathbf{X})$, as the exact reconstruction of \mathbf{X} may be impractical. The relaxation formulation is:

$$\min_Q \mathcal{L}_{SE} = \|\mathbf{X} - Q\mathbf{X}\|_F^2 + \lambda_1 \|Q\|_F^2, \text{ s.t. } \text{diag}(Q) = 0, \quad (3)$$

where λ_1 is a weight hyperparameter of optimization.

Step 3: Generating latent homophilic structure. We construct the latent homophilic structure S^* by $Q + Q^T$, while this structure still has noise and outliers. Therefore, we rely on Algorithm 1 to generate S^* . Specifically, the SVD decomposition in Algorithm 1 aims to filter noisy information during the structure generation. In each iteration, we refine the latent structure S^* . We employ the scalable randomized SVD (Halko, Martinsson, and Tropp 2011) to improve the computation efficiency for large-scale graphs. Details are available in Appendix 2.1.

Algorithm 1: The generation algorithm of S^*

Input: Coefficient matrix Q , subspaces dimension $K = 4$, rank $r = Kd + 1$, where d is the number of node classes.

Output: Latent structure S^* .

- 1: **Initialization:** $Q' = \frac{1}{2}(Q + Q^T)$.
- 2: **Compute:** the r rank SVD of Q' via $Q' = U\Sigma V^T$.
- 3: **Compute:** $L = U\Sigma^{\frac{1}{2}}$ and normalize each row of L .
- 4: **Update:** $L' \leftarrow$ set the negative values in L to zero.
- 5: **Obtain:** $S^* = (L' + L'^T) / \|L\|_\infty$, where $s_{ij} \in [0, 1]$.

Dual-view Contrastive Learner. So far we have obtained the latent structure S^* , and in the previous step, we focus on learning S^* based on the node features. To refine such a structure, we further explore the enriched structural information of the graph and propose a novel dual-view contrastive learner. We take four steps for such a refinement. **Step 1: Generating the dual views of latent structure.** We

denote the graph as $G = (S^*, \mathbf{X})$, where S^* is the learnable latent homophilic structure. Based on G , we generate two graphs G_1 and G_2 via the corruption function (Velickovic et al. 2019) to refine the structure in a self-supervised manner. Specifically, the corruption function randomly removes a small portion of edges from S^* and also randomly masks a fraction of dimensions with zeros in node features \mathbf{X} .

Step 2: Aggregating information on latent structure. For efficient aggregation on S^* , we devise a truncated threshold GCN to control the sparsity of the structure. For S^* , we introduce a threshold σ to decide if there exists a soft connection with continuous values between two nodes and then form a new structure S^*_σ . Such a way is quite different from the previous hard-coding operations (Liu et al. 2022) that only have 0 or 1, and our S^*_σ can be flexibly applied to various benchmarks. We employ the truncated threshold GCN on three graphs, including G , G_1 , and G_2 . The proposed truncated threshold GCN on graph G can generate the representations as follows:

$$S^* = \{s_{ij}^* \geq \sigma \mid s_{ij}^* \in S^*\} \quad (4)$$

$$Z = \text{GCN}(\mathbf{X}, S^*) = \hat{S}^* \text{ReLU}(\hat{S}^* \mathbf{X} W^{(0)}) W^{(1)}$$

where ReLU is an activation function, $W^{(0)}$ and $W^{(1)}$ are the trainable weight matrices, $\hat{S}^* = S^* + I$, $I \in \mathbb{R}^{|V| \times |V|}$ is the identity matrix and the degree diagonal matrix \tilde{D}_{ii} with $\tilde{D}_{ii} = \sum_{j \in V} \tilde{S}_{ij}^*$, $\forall i \in V$. We set $\hat{S}^* = \tilde{D}^{-\frac{1}{2}} \tilde{S}^* \tilde{D}^{-\frac{1}{2}}$. $W^{(0)}$ and $W^{(1)}$ are trainable parameter matrices of GCN. Z_1 and Z_2 denote the node embedding matrices for the two views G_1 and G_2 , and these node embeddings are generated from the proposed GCN encoder.

Step 3: Sampling the contrastive samples. For a node $v_i \in V$, let us denote the corresponding nodes in G_1 and G_2 as $G_1(v_i)$ and $G_2(v_i)$ respectively. Then we introduce the node-pair sampling rules for the contrastive learning as follows: a) **positive example** is the node pair from the same node of different graph views, that is, $\forall i \in V$, the pair $(G_1(i), G_2(i))$. b) **negative example** is the node pair from the different nodes of the same or different graph views, that

is, $\forall i \in V, V_{-i} = \{j \in V \mid j \neq i\}$. Both $(G_1(i), G_1(j))$ and $(G_1(i), G_2(j))$ are the negative examples.

Step 4: Optimizing the contrastive loss. In addition to the above dual-view optimization, we also propose a novel pairwise constraint to optimize the original graph view, which can further improve the quality of the learned homophilic structure. Specifically, we sample the node pairs from the training set with labels. The same-class node pairs are positive samples noted as (u, v) , while the different-classes node pairs are negative samples noted as (u, v_n) , where u, v , and v_n belong to the training node set and $y(u) = y(v)$, $y(u) \neq y(v_n)$. Here $y(\cdot)$ is the node label. We formally propose the loss function as:

$$\begin{aligned} \mathcal{L}_{refine} = & \sum_{i \in V} \left[-\frac{\cos(z_{1i}, z_{2i})}{\tau} \right. \\ & \left. + \log \left(\sum_{j \in V_{-i}} e^{\frac{\cos(z_{1i}, z_{1j})}{\tau}} + e^{\frac{\cos(z_{1i}, z_{2j})}{\tau}} \right) \right] \\ & - \lambda_2 [\log(\sigma(z_u^\top z_v)) - \log(\sigma(-z_u^\top z_{v_n}))] \end{aligned} \quad (5)$$

where z_{1i} and z_{2i} denote embeddings node i on Z_1 and Z_2 respectively, $z_{(v)}$ denotes embedding of node v on Z , $\cos(\cdot)$ is the cosine similarity between the two embeddings, τ is a temperature parameter, and λ_2 is a hyperparameter of the second term. The first term of Eq. 5 encourages the consistent information between positive samples, while the second term penalizes the inconsistent information between dual views. The last term of Eq. 5 makes sure that the same-class nodes have more similar representations.

Structure Refinement. The node embedding matrix \mathbf{Z} generated by Eq. 5 has incorporated the refined structure and node features. Finally, we feed \mathbf{Z} into the structure inducer again to iteratively refine the structure S^* . Equipped with both the original graph A and the refined one S^* , we use a structure bootstrapping mechanism $S^* \leftarrow \zeta A + (1 - \zeta)S^*$ to update S^* with a slow-moving of A , where ζ is a hyperparameter to balance the information between A and S^* . Specifically, the input graphs with high heterophily will lead to smaller ζ , while the ones with high homophily have larger ζ . By doing so, we can reduce the scale of “right-shift” over heterophilic graphs and thus potentially mitigate the structural OOD issue under malicious attacks as discussed in Fig. 1 in the Introduction Section.

Graph Encoder

Our graph encoder consists of a GCN encoder and a GCN decoder, where the former encodes the masked features, and the latter aims to generate the reconstructed features $\hat{\mathbf{X}}$. We feed the masked node features $\tilde{\mathbf{X}}$ and S^* to the graph encoder. Then we use a scaled cosine error to optimize the encoder as follows:

$$\mathcal{L}_{Re} = \frac{1}{|\tilde{\mathcal{V}}|} \sum_{v_i \in \tilde{\mathcal{V}}} \left(1 - \frac{\mathbf{x}_i^\top \hat{\mathbf{x}}_i}{\|\mathbf{x}_i\| \cdot \|\hat{\mathbf{x}}_i\|} \right)^\gamma, \gamma \geq 1 \quad (6)$$

where \mathbf{x}_i and $\hat{\mathbf{x}}_i$ are the feature and reconstructed feature of node i , γ is a scale factor.

Classifier and Loss Functions

Finally, our classifier outputs predictions. We generate classification representations via a fully-connected layer $F(\cdot)$, that is $y_{\text{pred}} = \text{softmax}(F(\mathbf{h}_i))$. Then the loss of the classifier can be expressed as $\mathcal{L}_{Pre} = \sum_{i=1}^{N_i} y_i \log y_{\text{pred } i}$. We jointly train the graph encoder and classifier with \mathcal{L} , which can be expressed as:

$$\mathcal{L} = \mathcal{L}_{Pre} + \beta \mathcal{L}_{Re} \quad (7)$$

where β is a hyperparameter of loss weight.

Experiments

Datasets, Baselines and Settings

Datasets: We experiment on nine benchmarks. For six heterographic spatial datasets including **Cornell**, **Texas**, **Wisconsin** (Pei et al. 2020), **Chameleon**, **Squirrel** (Rozemberczki, Allen, and Sarkar 2021), nodes are web pages and edges are hyperlinks between these pages, and **Actor** (Tang et al. 2009), nodes are actors and edges denote co-occurrences on same web pages. For the three homophilic datasets including **Cora**, **Citeseer** and **PubMed** (Yang, Cohen, and Salakhudinov 2016), nodes refer to articles, and edges are the citations between articles. Due to space limitations, we provide detailed descriptions in Appendix 4.1.

Baselines: We follow the previous works (Jin et al. 2021b; He et al. 2022) to use eleven baselines. We categorize these methods into three groups: **1) multi-hop-based approaches** MixHop (Abu-El-Haija et al. 2019) and H2GCN (Zhu et al. 2020a), which mix the multi-hop neighbors for aggregation; **2) ranking-based approaches** NLGNN (Liu, Wang, and Ji 2021), GEOM-GCN (Pei et al. 2020), Node2Seq (Yuan and Ji 2021) and GPNN (Yang et al. 2022) that aim to search on the network structure and then perform selective aggregation; **3) structure learning approaches** ProGNN (Jin et al. 2020), UGCN (Jin et al. 2021a), BM-GCN (He et al. 2022) and GREET (Liu et al. 2023) that automatically learn graph structures for aggregations. Specifically, **ProGNN** preserves the low-rank and sparsity characteristics of the graph structure for robust GCN. **UGCEN** and **Simp-GCN** employ a similarity preservation scheme for structure learning on heterophilic graphs and **BM-GCN** employs a selective aggregation on structure via a block-guided strategy. We also compare our model with a recently proposed spectral-based method ALT-GCN (Xu et al. 2023).

Settings: We implement our method by Pytorch and Pytorch Geometric and use Adam Optimizer on all datasets with the learning rate as 0.001. We configure epochs as 1000 and apply early stopping with the patience of 40. We configure the hidden size as 64 and the batch size as 256. We perform the structure learning for 2 rounds. More detailed hyperparameters are available in Appendix 4.3.

Main Results

Comparisons under Poisoning Attacks. We compare the robustness of our LHS with five baseline approaches under a popular poisoning attack (Jin et al. 2020) on three

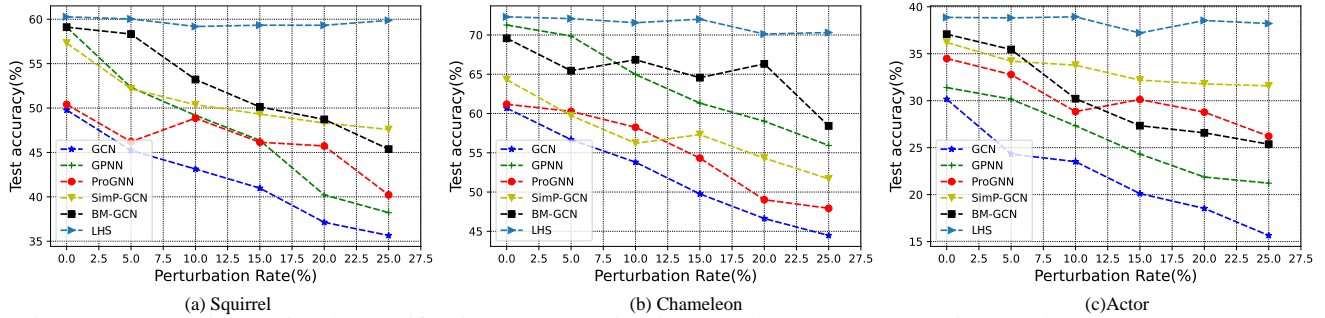


Figure 4: Comparisons of node classification under a poisoning attack. We repeat three times and report the mean values.

Table 1: Robustness comparisons in terms of classification accuracy (%) under 2 evasion-based attacks OOD and Injected.

	Wisconsin		Texas		Chameleon		Squirrel		Actor		average
	OOD	Injected	OOD	Injected	OOD	Injected	OOD	Injected	OOD	Injected	
H2GCN	48.24±2.1	41.53±1.7	45.33±0.9	39.86±1.1	47.20±1.5	37.21±2.3	48.27±3.1	36.34±1.6	21.33±2.3	14.17±1.4	37.97
GPNN	52.78±0.8	40.21±1.4	56.33±1.1	38.78±1.9	54.62±2.0	48.49±1.6	50.23±0.6	40.55±1.3	20.83±2.7	16.28±1.5	41.91
UGCN	72.37±2.7	44.58±2.2	50.40±1.5	41.92±0.7	57.23±3.1	40.39±2.8	52.45±3.3	41.79±3.2	23.37±1.9	15.57±0.8	44.00
SimP-GCN	73.34±2.1	61.43±2.4	59.76±3.3	60.31±0.4	61.28±1.6	54.57±2.6	54.34±1.0	54.01±2.3	28.96±1.8	24.31±2.9	53.23
BM-GCN	76.58±0.5	69.78±1.3	62.17±1.1	63.22±1.0	62.37±2.6	52.58±2.3	57.30±1.0	59.82±0.7	26.17±1.4	18.92±1.9	54.89
LHS	82.31±0.5	73.34±1.1	71.15±1.4	68.19±1.6	67.33±0.9	60.10±2.2	68.76±3.1	62.13±2.7	32.23±2.6	33.42±1.8	62.41

benchmarks including Squirrel, Chameleon, and Actor. Under various perturbation rates ranging from 0 to 25%, Figure 4 shows that our LHS consistently performs best among all baselines. For example, ours yields higher classification accuracy of up to 20 points compared to ProGNN. These results confirm the superiority of our latent structure learning scheme against poisoning attacks. The existing structure learning methods, including BM-GCN, SimP-GCN, and ProGNN, are also extremely vulnerable under large positioning perturbations. Nevertheless, they are better than the other two, showing the promise of structure learning over heterophilic graphs. We also observe that the positioning perturbations, which can significantly degrade the baselines at a large rate (i.e., 25%), have a very slight impact on our method. We attribute such gains to the latent structure that can be resistant to the structural OOD issue discussed in the Introduction Section, which will also be illustrated in the first question of the Discussion Section.

Comparisons under Evasion Attacks. We presented two evasion-based attacks (Zhang et al. 2016), i.e., “OOD evasion attack (OOD)” and “injected evasion attack (Injected)” in Fig. 1 (b) and Fig. 1(c), to craft attack samples with destructive structural perturbations to the edges of the graph. Here we compare our method with five baselines on five heterophilic graphs, and report the results in Table 1. We chose these five baselines because they are representative of different types of GCN and have been widely used in previous studies. For two nodes with different classes, the “Injected” attacks manipulate to inject a connection with a 0.9 probability. We repeat our experiments three times and report the mean and variance values in Table 1. Under the two attacks, Table 1 shows that our method consistently achieves the best among all baselines on five benchmarks. Compared with “OOD” attacks, “Injected” attacks are much more constructive as they significantly increase of heterophily of the testing set. Compared to the state-of-the-art structure learn-

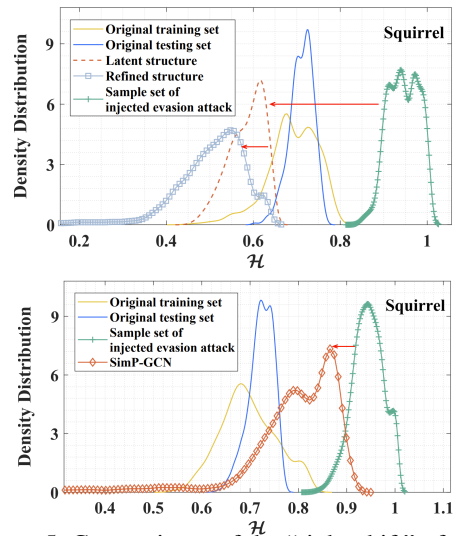


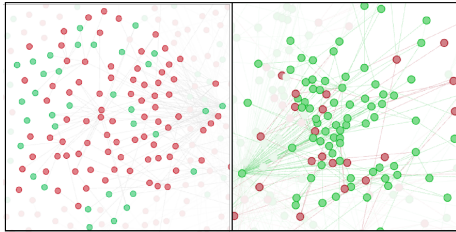
Figure 5: Comparisons of the “right-shift” of \mathcal{H}_E .

ing method BM-GCN, our LHS achieves an 11.33 point accuracy under “OOD” attacks. Overall, these results suggest that LHS is more robust against both attacks compared to all the considered baselines. The key to these improved results is the ability of our LHS to perform global searches of the homophilic structure learned by the structure inducer.

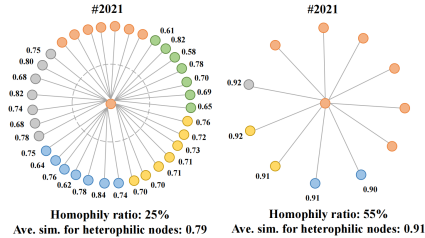
Comparisons without attacks. We have shown that our model is more robust than existing methods under various attacks. To further investigate the performance without attacks, we conduct experiments on the five heterophilic graphs and compare ours with baseline approaches. Table 2 shows that the proposed LHS performs best and we attribute this to the information aggregation in a homophilic way on heterophilic graphs. Additionally, we also achieve better or comparable classification results on three benchmarks for homophilic graphs. This suggests that improving homophily for both homophilic and heterophilic graphs benefits node classification, and this also remotely aligns with a

Table 2: Comparisons of node classification without any attacks.

	Wisconsin	Texas	Cornell	Chameleon	Squirrel	Actor	Cora	Citeseer	Pubmed	Average
MixHop	75.88±4.9	77.84±7.7	73.51±6.2	60.50±2.5	43.80±1.4	32.22±2.3	81.90±0.8	71.40±1.3	80.80±0.6	66.43
H2GCN	86.67±4.6	84.86±6.7	82.16±6.0	57.11±1.6	37.90±2.0	35.86±1.0	87.81±1.3	77.07±1.6	89.59±0.3	71.00
NLGNN	87.30±4.3	85.40±3.8	84.90±5.7	70.10±2.9	59.00±1.2	37.90±1.3	88.50±1.8	76.20±1.6	88.20±0.5	75.28
GEOM-GCN	65.10±6.5	67.84±5.8	60.00±6.5	65.81±1.6	45.49±1.3	31.94±1.0	85.65±1.7	79.41±1.7	90.49±0.3	65.75
Node2Seq	60.30±7.0	63.70±6.1	58.70±6.8	69.40±1.6	58.80±1.4	31.40±1.0	-	-	-	57.05
GPNN	86.86±2.6	85.23±6.4	85.14±6.0	71.27±1.8	59.11±1.3	37.08±1.4	-	-	-	70.79
UGCN	69.89±5.2	71.72±6.2	69.77±6.7	54.07±1.7	34.39±1.9	-	84.00±0.9	74.08±1.2	85.22±0.7	67.89
SimP-GCN	85.49±3.5	81.62±6.5	84.05±5.3	-	-	36.20±1.3	-	-	-	71.84
BM-GCN	-	85.13±4.6	-	69.58±2.9	51.41±1.1	-	87.99±1.2	76.13±1.9	90.25±0.7	-
GREET	84.90±3.3	87.00±4.2	85.10±4.9	63.60±1.2	42.30±1.3	36.60±1.2	83.81±0.9	73.08±0.8	80.29±1.0	70.74
ALT-GCN	76.40±3.9	70.90±4.3	73.90±5.1	65.80±0.9	52.40±0.8	-	81.20±0.5	71.40±0.4	79.10±0.9	71.39
LHS	88.32±2.3	86.32±4.5	85.96±5.1	72.31±1.6	60.27±1.2	38.87±1.0	88.71±0.7	78.53±1.5	87.65±0.3	76.34



(a) visualization of a local structure on squirrel



(b) visualization of a node connection on squirrel

Figure 6: The visualization of the latent structure learned by the proposed LHS.

previous work (Yan et al. 2021), showing that our method can handle both types of graphs in a unified manner.

Discussion

Can LHS reduce the scale of “right-shift” of \mathcal{H} distributions? We have discussed that the “right-shift” phenomenon, i.e., the structural OOD, is the cause of performance degradation under attacks in the Introduction Section. To answer this question, we visualize how our method reduces the “right-shift” for experiments in Table 1 on Squirrel. Under the “injected evasion attack”, Figure 5 shows that our latent structure can greatly move the \mathcal{H} distribution of the attacking sample to the left, thus reducing the “right-shift” (see the red arrow). We also observe that the second round of refinement can further move distribution to the left side, further improving the model’s robustness. However, we find that existing SimP-GCN can slightly move the distribution, visually explaining why LHS is more robust than SimP-GCN. This further confirms our hypothesis that reducing “right-shift” can harden the GCN over heterophilic graphs.

What does the learnable homophilic structure look like?

For this question, we rely on a tool Gephi (Bastian, Heymann, and Jacomy 2009) to visualize the structure of the test set of Squirrel and the homophilic structure of LHS, with a truncated threshold σ set as 0.91. Figure 6(a) demonstrates the visualizations of the two structures respectively. We can observe that there are many more homophilic edges in our structure, compared with the one of the original test set. We also study the connection of the node #2021 of Squirrel. Figure 6(b) shows that the homophily ratio, which is computed by $1 - \mathcal{H}v_{2021}$, is significantly increased from 25% to 55% after the structure latent learning. In this case, we observe that our model reduces the heterophilic connections, while keeping the homophilic edges unchanged.

Can the learnable homophilic structure be applied to

other tasks? To answer this question, we also apply the homophilic structure learned on four graphs, including Wisconsin, Squirrel, Chameleon, and Cora, to the graph clustering task. We use vanilla GCN (Kipf and Welling 2017) and the proposed structure inducer of LHS to develop “GCN + Structure Inducer”. Even on the vanilla GCN, Table 3 shows that our “GCN + Structure Inducer” outperforms all other baselines on heterophilic graphs. For example, ours outperforms the SimP-GCN on Squirrel by 2.79 points. We attribute such again to our homophilic structure.

Table 3: Performance Comparisons on graph clustering

	Wisconsin	Squirrel	Chameleon
SimP-GCN	58.42	38.57	46.44
BMGCN	54.92	40.26	50.17
AGC	43.71	32.98	35.78
GCN + Structure Inducer	61.32	41.36	52.37

Conclusion

This paper studies robust graph convolution networks over heterophilic graphs. We take the first step towards quantitatively analyzing the robustness of GCN approaches over omnipresent heterophilic graphs for node classification, and reveal that the vulnerability is mainly caused by the structural out-of-distribution (OOD). Based on this crucial observation, we present LHS, a novel method that aims to harden GCN against various attacks by learning latent homophilic structures on heterophilic graphs. Our LHS can iteratively refine the latent structure during the learning process, facilitating the model to aggregate information in a homophilic way on heterophilic graphs. Extensive experiments on various benchmarks show the effectiveness of our approach. We believe our structure can also benefit more graph tasks for better representation learning. Future work could focus on the development of novel adversarial training methods based on the structural OOD.

Acknowledgments

This work was partially supported by the National Key R&D Program of China (Grant No.2022YFB2902200), Major Projects of National Natural Science Foundation of China (Grant No.72293583), and the Joint Funds for Regional Innovation and Development of the National Natural Science Foundation of China (No. U21A20449).

References

- Abu-El-Haija, S.; Perozzi, B.; Kapoor, A.; Alipourfard, N.; Lerman, K.; Harutyunyan, H.; Ver Steeg, G.; and Galstyan, A. 2019. Mixhop: Higher-order graph convolutional architectures via sparsified neighborhood mixing. In *international conference on machine learning*, 21–29. PMLR.
- Bastian, M.; Heymann, S.; and Jacomy, M. 2009. Gephi: an open source software for exploring and manipulating networks. In *Proceedings of the international AAAI conference on web and social media*, volume 3.
- Biggio, B.; Corona, I.; Maiorca, D.; Nelson, B.; Šrncić, N.; Laskov, P.; Giacinto, G.; and Roli, F. 2013. Evasion attacks against machine learning at test time. In *Joint European conference on machine learning and knowledge discovery in databases*. Springer.
- Bo, D.; Wang, X.; Shi, C.; and Shen, H. 2021. Beyond low-frequency information in graph convolutional networks. In *Proceedings of the AAAI Conference on Artificial Intelligence*, volume 35, 3950–3957.
- Böttcher, A.; and Wenzel, D. 2008. The Frobenius norm and the commutator. *Linear algebra and its applications*, 429(8-9): 1864–1885.
- Cavallari, S.; Cambria, E.; Cai, H.; and Chang, K. 2019. Embedding both finite and infinite communities on graphs. *IEEE computational intelligence magazine*, 14(3): 39–50.
- Dai, H.; Li, H.; Tian, T.; Huang, X.; Wang, L.; Zhu, J.; and Song, L. 2018. Adversarial attack on graph structured data. In *International conference on machine learning*, 1115–1124. PMLR.
- Halko, N.; Martinsson, P.-G.; and Tropp, J. A. 2011. Finding structure with randomness: Probabilistic algorithms for constructing approximate matrix decompositions. *SIAM review*, 53(2): 217–288.
- Hamilton, W. L.; Ying, Z.; and Leskovec, J. 2017. Inductive Representation Learning on Large Graphs. In *NIPS*.
- He, D.; Liang, C.; Liu, H.; Wen, M.; Jiao, P.; and Feng, Z. 2022. Block modeling-guided graph convolutional neural networks. In *Proceedings of the AAAI conference on artificial intelligence*, volume 36, 4022–4029.
- Jin, D.; Yu, Z.; Huo, C.; Wang, R.; Wang, X.; He, D.; and Han, J. 2021a. Universal graph convolutional networks. *Advances in Neural Information Processing Systems*, 34: 10654–10664.
- Jin, W.; Derr, T.; Wang, Y.; Ma, Y.; Liu, Z.; and Tang, J. 2021b. Node similarity preserving graph convolutional networks. In *Proceedings of the 14th ACM international conference on web search and data mining*, 148–156.
- Jin, W.; Ma, Y.; Liu, X.; Tang, X.; Wang, S.; and Tang, J. 2020. Graph structure learning for robust graph neural networks. In *Proceedings of the 26th ACM SIGKDD international conference on knowledge discovery & data mining*, 66–74.
- Kipf, T. N.; and Welling, M. 2016. Variational graph auto-encoders. *arXiv preprint arXiv:1611.07308*.
- Kipf, T. N.; and Welling, M. 2017. Semi-Supervised Classification with Graph Convolutional Networks. In *International Conference on Learning Representations*.
- Li, H.; Xu, W.; Qiu, C.; and Pei, J. 2022. Fast Markov clustering algorithm based on belief dynamics. *IEEE Transactions on Cybernetics*.
- Li, S.; Kim, D.; and Wang, Q. 2023. Restructuring Graph for Higher Homophily via Adaptive Spectral Clustering. In *Proceedings of the AAAI Conference on Artificial Intelligence*, volume 37, 8622–8630.
- Lin, W.; Lan, H.; and Li, B. 2021. Generative Causal Explanations for Graph Neural Networks. In *Proceedings of the 38th International Conference on Machine Learning*.
- Liu, M.; Wang, Z.; and Ji, S. 2021. Non-local graph neural networks. *IEEE Transactions on Pattern Analysis and Machine Intelligence*.
- Liu, Y.; Zheng, Y.; Zhang, D.; Chen, H.; Peng, H.; and Pan, S. 2022. Towards unsupervised deep graph structure learning. In *Proceedings of the ACM Web Conference 2022*, 1392–1403.
- Liu, Y.; Zheng, Y.; Zhang, D.; Lee, V. C.; and Pan, S. 2023. Beyond smoothing: Unsupervised graph representation learning with edge heterophily discriminating. In *Proceedings of the AAAI conference on artificial intelligence*, volume 37, 4516–4524.
- Luan, S.; Hua, C.; Lu, Q.; Zhu, J.; Zhao, M.; Zhang, S.; Chang, X.-W.; and Precup, D. 2022. Is Heterophily A Real Nightmare For Graph Neural Networks on Performing Node Classification?
- Pei, H.; Wei, B.; Chang, K. C.-C.; Lei, Y.; and Yang, B. 2020. Geom-GCN: Geometric Graph Convolutional Networks. In *International Conference on Learning Representations*.
- Qiu, C.; Geng, Y.; Lu, J.; Chen, K.; Zhu, S.; Su, Y.; Nan, G.; Zhang, C.; Fu, J.; Cui, Q.; et al. 2023. 3D-IDS: Doubly Disentangled Dynamic Intrusion Detection. In *Proceedings of the 29th ACM SIGKDD Conference on Knowledge Discovery and Data Mining*, 1965–1977.
- Qiu, C.; Huang, Z.; Xu, W.; and Li, H. 2022a. Fast Community Detection based on Graph Autoencoder Reconstruction. In *2022 7th International Conference on Big Data Analytics (ICBDA)*, 265–271. IEEE.
- Qiu, C.; Huang, Z.; Xu, W.; and Li, H. 2022b. VGAER: graph neural network reconstruction based community detection. *arXiv preprint arXiv:2201.04066*.
- Rozemberczki, B.; Allen, C.; and Sarkar, R. 2021. Multi-scale attributed node embedding. *Journal of Complex Networks*, 9(2): cnab014.

- Suresh, S.; Budde, V.; Neville, J.; Li, P.; and Ma, J. 2021a. Breaking the Limit of Graph Neural Networks by Improving the Assortativity of Graphs with Local Mixing Patterns. In *KDD*.
- Suresh, S.; Li, P.; Hao, C.; and Neville, J. 2021b. Adversarial graph augmentation to improve graph contrastive learning. *Advances in Neural Information Processing Systems*, 34: 15920–15933.
- Tang, J.; Sun, J.; Wang, C.; and Yang, Z. 2009. Social influence analysis in large-scale networks. In *Proceedings of the 15th ACM SIGKDD international conference on Knowledge discovery and data mining*, 807–816.
- Velickovic, P.; Fedus, W.; Hamilton, W. L.; Liò, P.; Bengio, Y.; and Hjelm, R. D. 2019. Deep graph infomax. *ICLR (Poster)*, 2(3): 4.
- Veličković, P.; Cucurull, G.; Casanova, A.; Romero, A.; Liò, P.; and Bengio, Y. 2018. Graph Attention Networks. In *International Conference on Learning Representations*.
- Wang, T.; Jin, D.; Wang, R.; He, D.; and Huang, Y. 2022a. Powerful Graph Convolutional Networks with Adaptive Propagation Mechanism for Homophily and Heterophily. In *Proceedings of the AAAI Conference on Artificial Intelligence*, volume 36, 4210–4218.
- Wang, Y.; and Derr, T. 2021. Tree decomposed graph neural network. In *Proceedings of the 30th ACM International Conference on Information & Knowledge Management*.
- Wang, Y.; Yi, K.; Liu, X.; Wang, Y. G.; and Jin, S. 2022b. ACMP: Allen-cahn message passing with attractive and repulsive forces for graph neural networks. In *The Eleventh International Conference on Learning Representations*.
- Xiong, T.; Qiu, C.; and Zhang, P. 2023. How ground-truth label helps link prediction in heterogeneous graphs. In *Proceedings of the 2023 2nd International Conference on Algorithms, Data Mining, and Information Technology*, 6–12.
- Xu, Z.; Chen, Y.; Zhou, Q.; Wu, Y.; Pan, M.; Yang, H.; and Tong, H. 2023. Node Classification Beyond Homophily: Towards a General Solution. In *Proceedings of the 29th ACM SIGKDD Conference on Knowledge Discovery and Data Mining*, 2862–2873.
- Yan, Y.; Hashemi, M.; Swersky, K.; Yang, Y.; and Koutra, D. 2021. Two sides of the same coin: Heterophily and over-smoothing in graph convolutional neural networks. *arXiv preprint arXiv:2102.06462*.
- Yang, L.; Li, M.; Liu, L.; bingxin niu; Wang, C.; Cao, X.; and Guo, Y. 2021. Diverse Message Passing for Attribute with Heterophily. In Beygelzimer, A.; Dauphin, Y.; Liang, P.; and Vaughan, J. W., eds., *Advances in Neural Information Processing Systems*.
- Yang, T.; Wang, Y.; Yue, Z.; Yang, Y.; Tong, Y.; and Bai, J. 2022. Graph pointer neural networks. In *Proceedings of the AAAI Conference on Artificial Intelligence*, volume 36, 8832–8839.
- Yang, Z.; Cohen, W.; and Salakhudinov, R. 2016. Revisiting semi-supervised learning with graph embeddings. In *International conference on machine learning*, 40–48. PMLR.
- Yuan, H.; and Ji, S. 2021. Node2Seq: Towards Trainable Convolutions in Graph Neural Networks. *CoRR*.
- Zhang, F.; Chan, P. P. K.; Biggio, B.; Yeung, D. S.; and Roli, F. 2016. Adversarial Feature Selection Against Evasion Attacks. *IEEE Transactions on Cybernetics*, 46.
- Zhang, K.; Zhang, Y.; and Cheng, H. 2020. Self-supervised structure learning for crack detection based on cycle-consistent generative adversarial networks. *Journal of Computing in Civil Engineering*, 34(3): 04020004.
- Zhang, X.; and Zitnik, M. 2020. GnnGuard: Defending graph neural networks against adversarial attacks. *Advances in neural information processing systems*, 33: 9263–9275.
- Zheng, X.; Liu, Y.; Pan, S.; Zhang, M.; Jin, D.; and Yu, P. S. 2022. Graph neural networks for graphs with heterophily: A survey. *arXiv preprint arXiv:2202.07082*.
- Zheng, Y.; Zhang, H.; Lee, V.; Zheng, Y.; Wang, X.; and Pan, S. 2023. Finding the Missing-half: Graph Complementary Learning for Homophily-prone and Heterophily-prone Graphs. *arXiv preprint arXiv:2306.07608*.
- Zhu, D.; Zhang, Z.; Cui, P.; and Zhu, W. 2019. Robust graph convolutional networks against adversarial attacks. In *Proceedings of the 25th ACM SIGKDD international conference on knowledge discovery & data mining*, 1399–1407.
- Zhu, J.; Jin, J.; Loveland, D.; Schaub, M. T.; and Koutra, D. 2022. How does heterophily impact the robustness of graph neural networks? theoretical connections and practical implications. In *Proceedings of the 28th ACM SIGKDD Conference on Knowledge Discovery and Data Mining*, 2637–2647.
- Zhu, J.; Yan, Y.; Zhao, L.; Heimann, M.; Akoglu, L.; and Koutra, D. 2020a. Beyond homophily in graph neural networks: Current limitations and effective designs. *Advances in Neural Information Processing Systems*, 33: 7793–7804.
- Zhu, Y.; Xu, Y.; Yu, F.; Liu, Q.; Wu, S.; and Wang, L. 2020b. Deep Graph Contrastive Representation Learning. *CoRR*.

Appendix

1. Structure Learning and “Right-Shift” Phenomenon

The “right-shift” of distribution, namely structural OOD, is caused by the high heterophilic neighbor structure, and learning the homophilic neighbor structure can be seen as one of the direct ways to “refrain from right-shift”. In this section, we provide the following analysis from a spectral perspective, aiming to bridge the gap between “refrain from right-shift” and structure learning, thus elaborating the rationale of LHS to improve classification robustness.

1.1. Theoretical Analysis

Given a graph signal \mathbf{x} defined on a graph G with normalized Laplacian matrix $L = I - \tilde{D}^{-\frac{1}{2}} \tilde{A} \tilde{D}^{-\frac{1}{2}}$, and the laplacian regularization term can be proposed as follows:

$$\mathbf{x}^T L \mathbf{x} = \frac{1}{2} \sum_{i,j} \tilde{A}_{ij} \left(\frac{\mathbf{x}_i}{\sqrt{1+d_i}} - \frac{\mathbf{x}_j}{\sqrt{1+d_j}} \right)^2. \quad (8)$$

where d_i and d_j denotes the degree of nodes v_i and v_j respectively. Thus a smaller value of $\mathbf{x}^T L \mathbf{x}$ indicates a more similar graph signal, i.e., a smaller signal difference between adjacent nodes. This laplacian regularization can also be seen as a smooth or average between two nodes signals (features). Specifically, from the perspective of graph signals optimization, we will show the relationship between GCN structure learning and the “right-shift” phenomenon.

Theorem 1. *From the perspective of graph signal optimization, the laplacian regularization of Eq. , is equivalent to the GCN convolutional operator, which is responsible for structure learning.*

Proof. First, the signal optimization with a laplacian regularization term can be formally proposed as follows:

$$\arg \min_{\mathbf{Z}} g(\mathbf{Z}) = \|\mathbf{Z} - \mathbf{X}\|^2 + \lambda \mathbf{X}^T L \mathbf{X}, \quad (9)$$

where \mathbf{Z} is the learned node embeddings, which can be used for downstream tasks such as node classification.

Then the gradient of $g(\mathbf{Z})$ at $\forall \mathbf{x} \in \mathbf{X}$ is calculated as:

$$\nabla g(\mathbf{x}) = 2(\mathbf{x} - \mathbf{x}) + 2\lambda L \mathbf{x}_0 = 2\lambda L \mathbf{x}_0. \quad (10)$$

And the one step gradient descent at $\forall \mathbf{x} \in \mathbf{X}$ with learning rate 1 is formulated as:

$$\begin{aligned} \mathbf{x} - \nabla g(\mathbf{x}) &= \mathbf{x} - 2\lambda L \mathbf{x} \\ &= (\mathbf{I} - 2\lambda L) \mathbf{x} \\ &= \left(\tilde{D}^{-\frac{1}{2}} \tilde{A} \tilde{D}^{-\frac{1}{2}} + L - 2\lambda L \right) \mathbf{x}. \end{aligned} \quad (11)$$

By setting λ to $\frac{1}{2}$, we finally arrives at:

$$\mathbf{x} - \nabla g(\mathbf{x}) = \tilde{D}^{-\frac{1}{2}} \tilde{A} \tilde{D}^{-\frac{1}{2}} \mathbf{x}. \quad (12)$$

□

The structure learning of the GCN convolution operator can be seen as a graph signal optimization with a laplacian regularization term. Hence, the graph convolution layer tends to **increase the feature similarity between the connected nodes**. Therefore, for heterophilic graphs, this structure learning will make neighbor heterophilic nodes have more similar embeddings, thus leading to poor classification performance. Based on this analysis, we introduce the rationality of our proposed LHS.

1.2. The Rationale behind LHS

In order to mitigate the “right-shift” phenomenon, which is caused by the GCN structure learning on inherent heterophilic structure, we propose LHS, a robust structure learning method on heterophilic graphs. It has the following two rationales that drew inspiration from the structural OOD problem:

- R1: For potential homophilic relationships, we aim to obtain the refined structure with more close homophilic connections, thus playing a positive role in the GCN structure learning.
- R2: For potential heterophilic relationships, our proposed LHS aims to suppress the negative edge connections, thus mitigating the “right-shift” phenomenon. We proposed a truncated threshold GCN to ensure that the negative edges with low confidence can preserve high similarity, thus mitigating the performance deterioration when GCN conducts structure learning.

The proposed LHS designs customized structure learning components to realize the above two rationales, which have not been completely considered by the existing structure learning methods. For example, the previous work (Jin et al. 2021a) (Jin et al. 2021b) considered the homophilic structure learning with high feature similarity, while they only utilize the pair-wise information of node features, i.e. kNN networks. Furthermore, they can not handle the potential heterophilic nodes which can hardly filter, while LHS proposes a truncated threshold GCN to only preserve the high-similarity connections, thus mitigating the performance deterioration.

1.3. The compatibility of LHS with sampling methods.

The proposed LHS is compatible with various sampling methods for contrastive learning. The positive instances and the negative instances, which are selected by a sampling method, can be fed into the contrastive learner to generate node representations. We follow the previous work (Zhu et al. 2020b) to use a popular sampling method in the proposed dual-view contrastive learner in our paper.

1.4. The graph tasks that could benefit from the proposed LHS

We additionally list the following tasks and give underlying reasons as follows.

- **GCN Model robustness** aims to protect the GCN models from various attacks. This task is under-explored on heterophilic graphs. The latent homophilic structure can effectively harden graph models when facing OOD or injected attacks.
- **Link prediction** aims to induce the edge relationships between nodes (Xiong, Qiu, and Zhang 2023). The latent homophilic structure learned by LHS captures the homophilic information of nodes and benefits the similar-feature-based link prediction tasks, such as similar product recommendations, and social recommendations with the same interests, etc.
- **High-order graph tasks** aim to make predictions on high-order structures, such as a community (Cavallari et al. 2019; Qiu et al. 2022a). The community is considered the smallest unit of prediction in these tasks and is hard to handle by the existing pairwise methods. The proposed latent homophilic structure can benefit these tasks by generating a refined latent structure.

1.5. Real-world example of the vulnerability of GCN models under malicious threats

Figure 1 (d) of the main paper demonstrates a malicious attack that can significantly degrade the classification accuracy of a system by 29.30%. We refer to the previous work (Zhu et al. 2020a) that involves real-world examples in fraud detection. We inject attacks, including malicious heterophilic nodes or spurious relations, into target nodes on a real-world social network, e.g., “the Actor”. Experimental results on “the Actor” in Table 1 of the main paper further confirm the vulnerability of GCN models under the above threats. We will follow the reviewer’s suggestion to include these examples to enhance the demonstration of the real-world value of our work.

2. The Complexity Analysis of LHS

We analyze the time and model complexity of LHS and provide some acceleration strategies.

2.1. Time Complexity

The time complexity of LHS mainly comes from the denoising SVD decomposition in the robust structure learner. A naive time complexity is $O(rN^2)$, where $r = 4K + 1 \ll N$, and K is the number of node classes. In general, the time complexity of LHS is $O(N^2)$, which is more suitable for the small dataset. For large-scale datasets, in order to balance time cost and performance, based on random projection principle (Halko, Martinsson, and Tropp 2011), we introduce the randomized SVD to further reduce the time complexity to $O(r \log(N)N)$, which is an acceptable complexity. Then, we can also generate the node representations within a local structure that consists of neighbor nodes instead of the computation throughout the whole graph

2.2. Model Complexity

For model complexity, benefit from the sampled learning strategy, for both robust structure learner and re-mask feature augementer, have high scalability for large-scale datasets, because they only need to employ contrastive learning or reconstructing on those sampled nodes features. One the other hand, the parameters introduced are always transforming the node feature dimension to a smaller dimension. To sum up, LHS only introduces additional parameters that is linear to the feature dimension.

3. Structural OOD Evidence

We provide more empirical evidence on structural OOD as well as the insights gained from interesting observation as follows.

3.1. Single-hop Layer

First, we show the empirical single-hop structural OOD observation on Wisconsin as Fig. 7, Squirrel as Fig. 8, Chameleon as Fig. 9, and the ‘right-shift’ of structural distribution can be seen between training set and test set; this structural OOD will lead to poor robustness. We also study the **counter example** of heterophilic graphs, as a homophilic graph, Cora can hardly be found the structural OOD problem in both four single-hop layers.

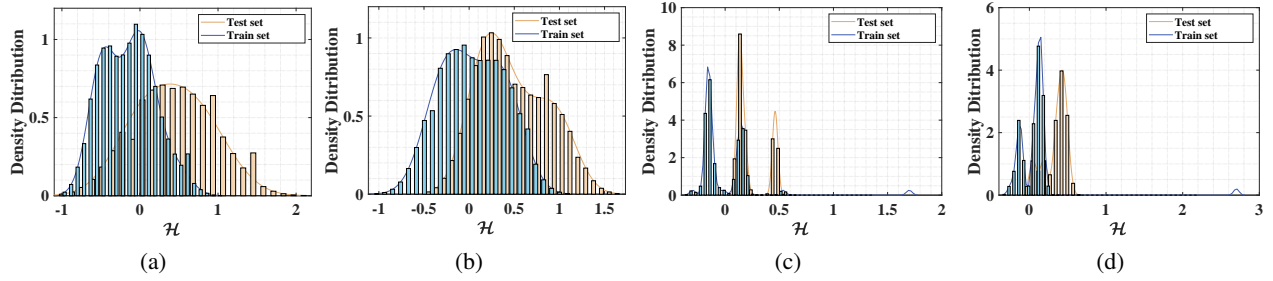


Figure 7: The ‘right-shift’ phenomons on the Wisconsin dataset.

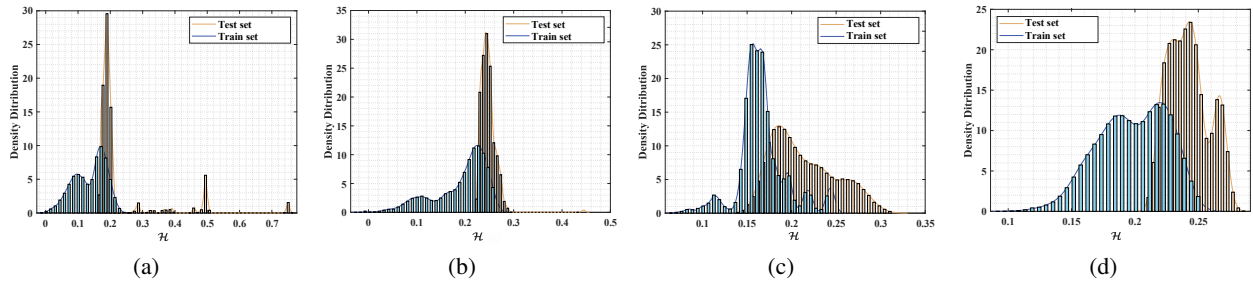


Figure 8: The ‘right-shift’ phenomons on the Squirrel dataset.

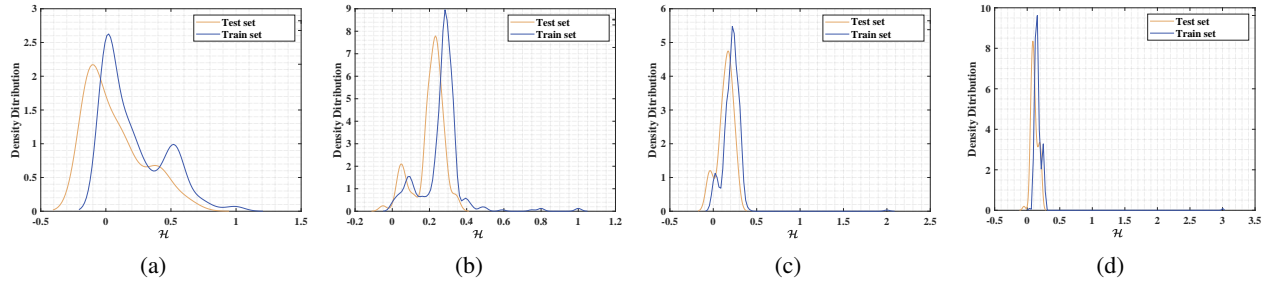


Figure 9: The ‘right-shift’ phenomons on the Chameleon dataset.

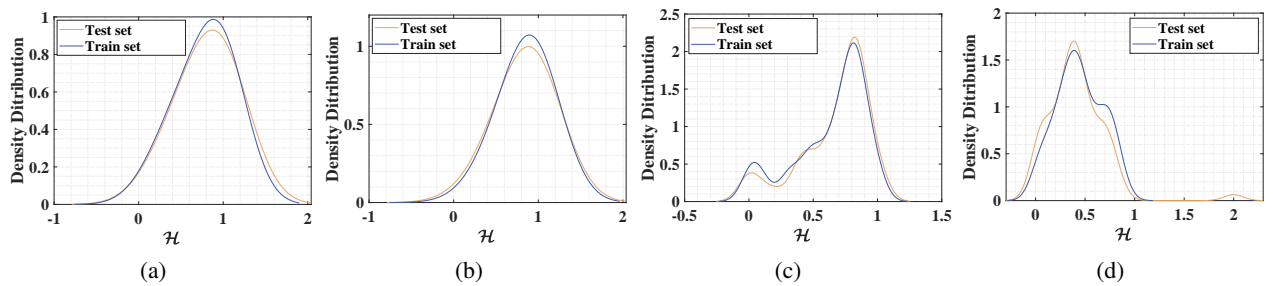


Figure 10: The counter-example Cora dataset, is free of the ‘right-shift’ phenomons.

3.2. Multi-hop Layer

We also provide the multi-hop joint distribution of edges (\mathcal{H}). The ‘right-shift’ edge distribution becomes more serious on heterophilic graphs that there is always a different degree of shift when each time we generate the distribution. While the homophilic graph Cora hardly exists the distribution shift, even the in multi-hop situation.

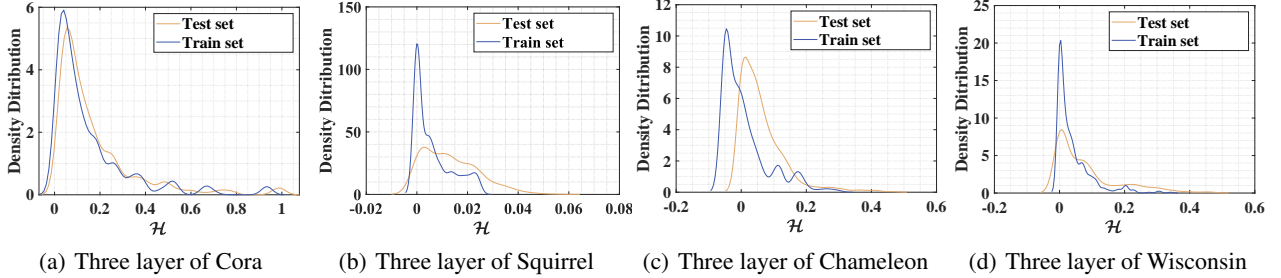


Figure 11: The multi-hop edge distribution on different datasets.

4. Experiments Details

4.1. Datasets Information

The statistical information about the eight real-world networks is given in Table 4, including the number of classes, the dimension of features, and the number of nodes and edges.

Table 4: Statistical information of eight real-world datasets.

Dataset	Cora	Citeseer	PubMed	Chameleon	Squirrel	Actor	Texas	Cornell
Classes	7	6	5	5	5	5	5	5
Features	1433	3703	500	2325	2089	932	1703	1703
Nodes	2708	3327	19717	2277	5201	7600	183	183
Edges	5278	4552	44324	31371	198353	26659	279	277

4.2. Split ratio of dataset.

For fair comparisons, we follow the settings of previous work (Pei et al. 2020) to use 60%, 20%, and 20% of the data for training, validation, and testing, respectively. Table 1 and Table 2 of the main paper report the comparison results under such settings.

4.3. Experiment Hardware and Setting

Hardware All experiments are performed on a Linux Machine with Intel(R) Xeon(R) Gold 6330 CPU with 28 cores, 378GB of RAM, and a NVIDIA RTX3090 GPU with 24GB of GPU memory.

Additional Setting We use Adam Optimizer with the $\beta_1 = 0.9, \beta_2 = 0.999, \epsilon = 1 \times 10^{-8}$ on all datasets. We run epochs $\in \{300, 1000\}$ with the learning rate $\in \{0.000005, 0.0001\}$ and apply early stopping with a patience of 40. We use PReLU as activation and the scaling factor $\tau \in \{0, 2\}$. According to the cross-entropy loss and ACC, we get a best model. On the validation set, we set hidden unit $\in \{16, 32\}$, learning rate $\in \{0.00005, 0.0001\}$, dropout in each layer $\in \{0.1, 0.2\}$ and the weight decay is $5e - 4$. Our method is implemented by Pytorch and Pytorch Geometric.

5. The Limitation of Previous Structure Learning Strategy

A large amount of current structure learning methods focus on the feature-level similarity to conduct structure learning (Jin et al. 2021a)(Jin et al. 2021b), which always formed poor similarity and can not reflect the true relationship between node pairs.

$$S_{ij} = \frac{\mathbf{x}_i^\top \mathbf{x}_j}{\|\mathbf{x}_i\| \|\mathbf{x}_j\|} \quad (13)$$

Now we provide empirical evidence to support our claim. To sum up, following the kNN method, we have calculated the cosine similarity on both homophilic graphs (Yang, Cohen, and Salakhudinov 2016) (Cora, Citeseer, Pubmed) and heterophilic

graphs (Pei et al. 2020) (Texas, Wiscon, Squirrel) as follows. We found that almost all node pairs that have formed bad similarities are only between 0.1 and 0.5. More seriously, there is no significant similarity difference between the same and different classes of nodes, whether they are between pairs or average levels. The results reveal that we can hardly distinguish nodes in different classes under such metrics and thus fail to learn a better structure to mitigate the “right-shift” phenomenon.

We respectively generate structures via the kNN network method and our proposed LHS. First, we compare the overall average similarity of the structures generated by the two methods; as shown in Fig. 12 to Fig. 15 (a), the average similarity of the LHS is between 0.6044 to 0.7844 on each dataset, while the average similarity of kNN networks only is 0.0562 to 0.3451. The (b) of Fig. 12 to Fig. 15 is the average similarity of sampled node and its homophilic (left) and heterophilic (right) neighbors (we sampled the same and enough neighbors to calculate the average similarity); and under the average level, the homophilic similarities are always higher than the heterophilic similarities constructed by RSGC (left), while getting closer to the ground-truth similarity. However, the similarity constructed by the kNN network (right) is poor and the heterophilic similarities are even higher than the homophilic similarities in Cora, Squirrel, and Chameleon, which makes the heterophilic nodes harder to distinguish, thus led poor structure learning effect. Note that the (b) from Fig. 12 to Fig. 15 represent the statistical similarity from the LHS (dark blue) and kNN network (light blue).

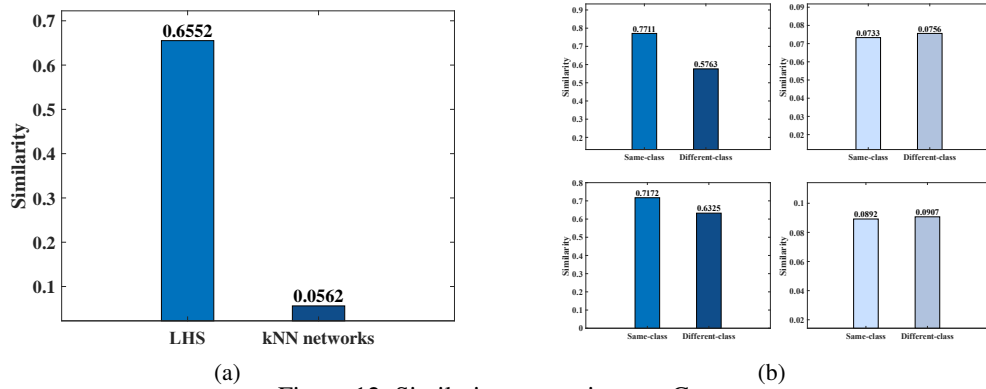


Figure 12: Similarity comparison on Cora.

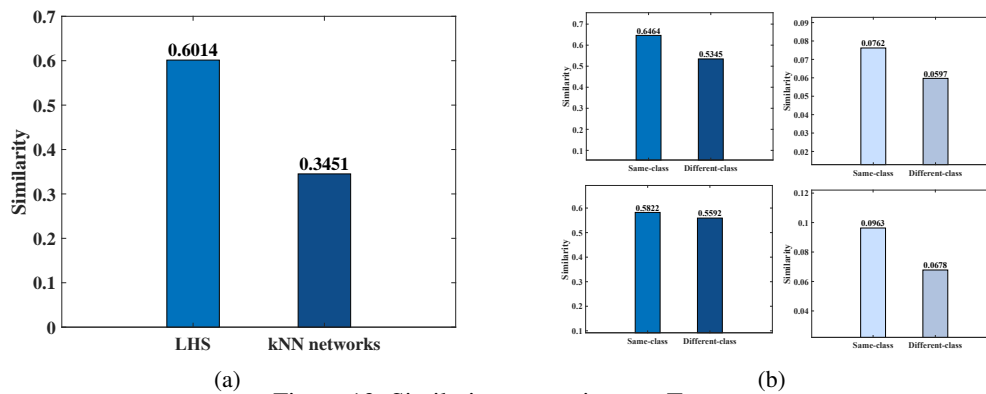
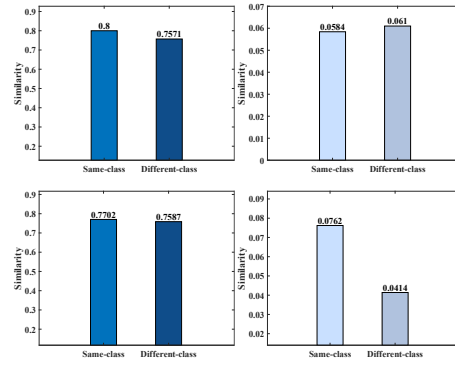
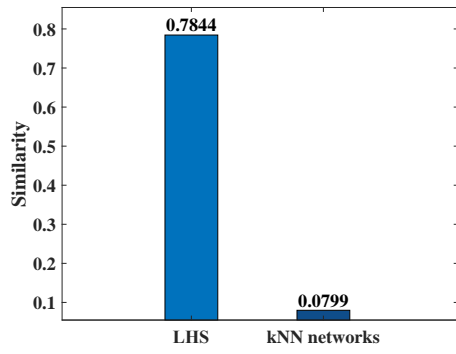
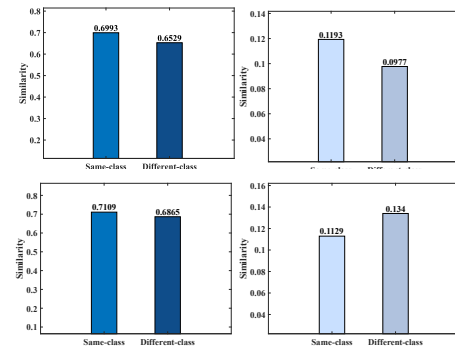
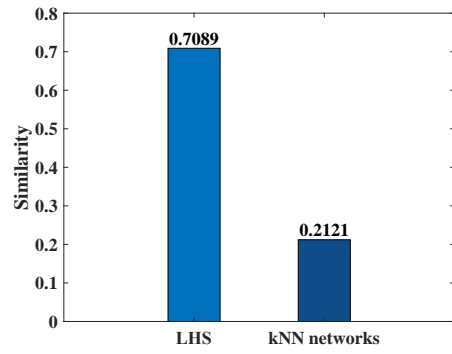


Figure 13: Similarity comparison on Texas.



(a) (b)
Figure 14: Similarity comparison on Squirrel.



(a) (b)
Figure 15: Similarity comparison on Chameleon.